Vol 18 No 3, March 2009
1674-1056/2009/18(03)/1096-09

Chinese Physics B

© 2009 Chin. Phys. Soc.
and IOP Publishing Ltd

Modelling of graded index waveguide fabricated by ion exchange on Er^{3+} doped glass*

Shao Gong-Wang(邵公望)† and Jin Guo-Liang(金国良)

Department of Physics, Shanghai Jiao Tong University, Shanghai 200240, *China*

(Received 8 April 2008; revised manuscript received 14 September 2008)

A general numerical tool, based on thermal diffusion equation and full-vectorial eigen-mode equation, has been presented for the systematic analysis of graded index channel waveguide fabricated by ion exchange on Er^{3+} doped glass. Finite difference method with full-vectorial formulation (FV-FDM) is applied to solving the full-vectorial modes of graded index channel waveguide for the first time. The coupled difference equations based on magnetic fields in FV-FDM are derived from the Taylor series expansion and accurate formulation of boundary conditions. Hybrid nature of vectorial guided modes for both pump (980 nm) and signal light (1550 nm) are demonstrated by the simulation. Results show that the fabrication parameters of ion exchange, such as channel opening width and time ratio of second step to first step in ion exchange, have large influence on the properties of waveguide. By optimizing the fabrication parameters, maintenance of monomode for signal light and improvement of the gain dynamics can be achieved in Er^{3+} doped waveguide amplifier (EDWA) fabricated by ion exchange technique. This theoretical model is significant for the design and fabrication of EDWA with ion exchange technique. Furthermore, a single polarization EDWA, which operates at wavelength from 1528 nm to 1541 nm for HE polarization, is numerically designed.

Keywords: graded index channel waveguide, finite difference method, full-vectorial mode, ion exchange technique

PACC: 4280L, 4110H, 4282, 6630J

1. Introduction

The refractive index profiles of optical waveguide are considered of two different types, step index and graded index profile. The optical channel waveguides based on graded index profile can be fabricated by thermal diffusion, ion implantation and ion exchange technique, such as Ti-diffused $LiNbO_3$, B^+-implanted fused silica, K^+–Na^+ exchanged glass, etc. The optical active and passive devices included graded index waveguides play an important role in optical information processing and telecommunication system. Optical waveguide amplifiers fabricated by ion exchange on Er^{3+} doped glasses (EDGs) have been attracting great interest for the last few years because of its compact structure, multi-channel integration and high ratio of performance to price.[1,2] Two-step ion exchange technique has been demonstrated as an attractive technology for the realization of Er^{3+} doped waveguide amplifiers (EDWAs) due to its simplicity, low cost, low birefringence and compatibility with monomode fibres.[3–5] A metallic stripe mask is deposited on the glass substrate before ion exchange. The ion exchange occurs at the unmasked region when glass substrate is immersed in molten salt of ions a (Ag^+ or K^+). In the first step of exchange, ions a are diffused into the substrate from molten salt, and ions b (Na^+) in glass are released to the molten salt to preserve charge neutrality. A surface channel waveguide with graded index profile is formed by thermal diffusion in the first step exchange. In the second step, the mask is removed, and the glass substrate is immersed in the molten salt of ions b. Then the ions a near the surface of substrate are exchanged back to the molten salt, and the distribution of ions a becomes more uniform in the substrate. In this way, the second step of exchange makes channel waveguide buried deeper in the substrate and form a more symmetrical graded index profile, which can obtain low propagation loss in waveguide and coupling loss with fibres.

The mode distribution of pump (980 nm) and signal light (1550 nm) propagating in Er^{3+} doped waveguide (EDW) depends on the index profile, which usually changes with the fabrication parameters, such as

*Project supported by the Foundation for Development of Science and Technology of Shanghai (Grant No 022261002).

†Corresponding author. E-mail: shaodog@sjtu.edu.cn

channel opening width (COW), time of first and second step ion exchange, etc.[3,4] Results reported in Refs.[2] and [6] show that the overlap factors about mode distribution of pump and signal light ($\Gamma_{\mathrm{p,s}}$) have great influence on the gain dynamics of EDWA fabricated by ion exchange technique. $\Gamma_{\mathrm{p,s}}$ have direct relations with the mode distribution of pump and signal light in EDWA. The performance of EDWA can be improved by optimizing the fabrication parameters. Accurate numerical calculation of the mode distribution and propagation constants for channel waveguide is indispensable to these optimizations. Among the various numerical techniques, e.g., finite difference method (FDM), finite element method (FEM) and imagery distance beam propagation method (ID-BPM), FDM is an attractive one because of the simplicity of its algorithm and the short computing time.[7] FDM based on scalar approximation is easy to realize. But it is not sufficiently accurate for the waveguides with polarization-dependent characteristics. In recent years, FDM based on full-vectorial formulation (FV-FDM) has been proposed to improve the accuracy and efficiency of mode field analysis in waveguide with step index profiles.[8−10] However, the studies about applying FV-FDM to the mode field analysis of channel waveguide with graded index profile have not yet been reported.

In this paper, we present a general numerical tool for the systematic analysis of graded index channel waveguide fabricated by ion exchange on EDG. The theoretical model is based on thermal diffusion equation and full-vectorial eigen-mode equation. FV-FDM is applied in the model to solve full-vectorial modes of graded index channel waveguide for the first time sofar as we know. The coupled difference equations based on magnetic fields in FV-FDM are derived from the Taylor series expansion and accurate formulation of boundary conditions. FV-FDM provides an accurate electromagnetic analysis on the mode distribution in graded index channel waveguide. Hybrid nature of vectorial guided modes for both pump and signal light is demonstrated by simulation. Then, the effective index and distribution of eigen-modes versus different fabrication parameters are numerically analysed. Results show that these parameters have large influence on the properties of waveguide. By optimizing the fabrication parameters, maintenance of monomode for signal light and improvement of the gain dynamics can be achieved in EDWA fabricated by ion exchange technique. This theoretical model is significant for the design and fabrication of EDWA with ion exchange technique. Finally, we numerically design a single polarization EDWA, which operates at the wavelength from 1528 to 1541 nm for HE polarization. And the working wavelength is changed with the fabrication parameters.

2. Theoretical model

2.1. Channel waveguide with two-dimensional graded index profile

In ion exchange technique, the relation between index profile and distribution of external ion in substrate (e.g., Ag^+ diffused into the glass substrate and exchanged with Na^+ in it) is approximatively linearity when the ion concentration is low.[4] Thus, the graded index profile after two-step ion exchange can be obtained from the ion (Ag^+) concentration distribution in substrate.

The diffusion process without external electric field is described by the two-dimensional diffusion equation, which takes the following form:[4,5]

$$\frac{\partial C_{\mathrm{Ag}}}{\partial t} = \nabla\left(\frac{D_{\mathrm{Ag}}}{1-\alpha C_{\mathrm{Ag}}}\nabla C_{\mathrm{Ag}}\right), \tag{1}$$

where C_{Ag} is the concentration of Ag^+ ion exchanged from molten salt into substrate, normalized with respect to the saturated concentration. D_{Ag} and D_{Na} are the self-diffusion coefficients of Ag^+ and Na^+, respectively, and $\alpha = 1 - D_{\mathrm{Ag}}/D_{\mathrm{Na}}$ is the relative transfer rate. Equation (1) can be solved numerically by Peaceman–Rachford method combined with the shooting method in Cartesian coordinates.[11] Cross section of buried channel waveguide is shown in Fig.1. The initial conditions and boundary conditions for two-step ion exchange process are expressed as follows:

$$\begin{cases} C^1_{t=0} = 0, \\ C^1_{|x|\le w/2;y=0;t} = 0, \\ \dfrac{\partial C^1_{|x|>w/2;y=0;t}}{\partial y} = 1, \\ C^1_{x;y=b;t} = 0, \\ C^1_{|x|=a/2;y;t} = 0; \end{cases} \qquad \begin{cases} C^2_{t=0} = C^1_{t=T_1}, \\ C^2_{x;y=0;t} = 0, \\ C^2_{x;y=b;t} = 0, \\ C^2_{|x|=a/2;y;t} = 0, \end{cases} \tag{2}$$

where $C^{1,2}$ are C_{Ag} in the first and second step ion exchange, respectively. T_1 is the time-length of first step exchange, w is the channel opening width, a and b are the width and depth of calculation region, re-

spectively.

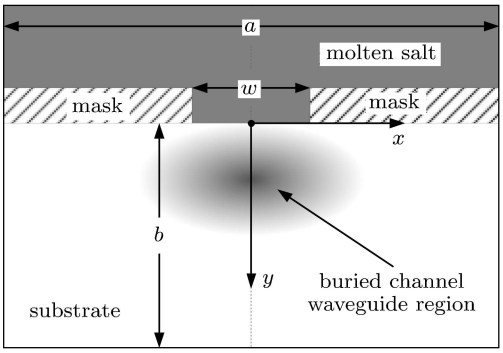


Fig.1. Cross section of buried channel waveguide fabricated by two-step ion exchange technique.

The graded index profile of cross section for channel waveguide after ion exchange can be expressed as a function of C_{Ag}:

$$n(x,y) = n_s + n_{\mathrm{Ag}} C_{\mathrm{Ag}}(x,y), \tag{3}$$

where n_s is the index of substrate before ion exchange n_{Ag} is the maximal increment in index of substrate resulting from $C_{\mathrm{Ag}} = 1$, determined experimentally.

2.2. Mode distribution in graded index waveguide

The vectorial wave equation for magnetic fields of guided wave can be derived from Maxwell's equations:

$$\nabla^2 \boldsymbol{H} + \left(\frac{\nabla \varepsilon_r}{\varepsilon_r}\right) \times \nabla \times \boldsymbol{H} + k_0^2 \varepsilon_r \boldsymbol{H} = 0, \tag{4}$$

where $\boldsymbol{H}$ is the magnetic field vector, k_0 is the wave number in free space, and $\varepsilon_r = n^2(x,y)$ is the relative electric permittivity of channel waveguide. In this model, the index profile of channel waveguide is assumed not to vary along the propagation direction (z direction), and we are concerned with the 2D cross-sectional analysis. Thus, the magnetic field vector can be written in a separable form:

$$\boldsymbol{H} = (H_x(x,y)\hat{\boldsymbol{x}} + H_y(x,y)\hat{\boldsymbol{y}} + H_z(x,y)\hat{\boldsymbol{z}})\mathrm{e}^{-\mathrm{j}\beta z}, \tag{5}$$

where β is the propagation constant of guided mode along the propagation direction.

Substituting Eq.(5) into Eq.(4), we can separate Eq.(4) into the x and y components:

$$\frac{\partial^2 H_x}{\partial x^2} + \frac{\partial^2 H_x}{\partial y^2} + k_0^2 \varepsilon_r H_x + \frac{1}{\varepsilon_r}\frac{\partial \varepsilon_r}{\partial y}\left(\frac{\partial H_y}{\partial x} - \frac{\partial H_x}{\partial y}\right) = \beta^2 H_x, \tag{6}$$

$$\frac{\partial^2 H_y}{\partial x^2} + \frac{\partial^2 H_y}{\partial y^2} + k_0^2 \varepsilon_r H_y - \frac{1}{\varepsilon_r}\frac{\partial \varepsilon_r}{\partial x}\left(\frac{\partial H_y}{\partial x} - \frac{\partial H_x}{\partial y}\right) = \beta^2 H_y. \tag{7}$$

The calculation region is then divided into small rectangular sub-regions of $\Delta x \times \Delta y$. In our finite difference approach, as shown in Fig.2, an arbitrary point P inside the mesh is in neighbourhood of points N, W, S, E. The relative electric permittivities for the sub-regions around point P are ε_{WN}, ε_W, ε_N, and ε_P, respectively.

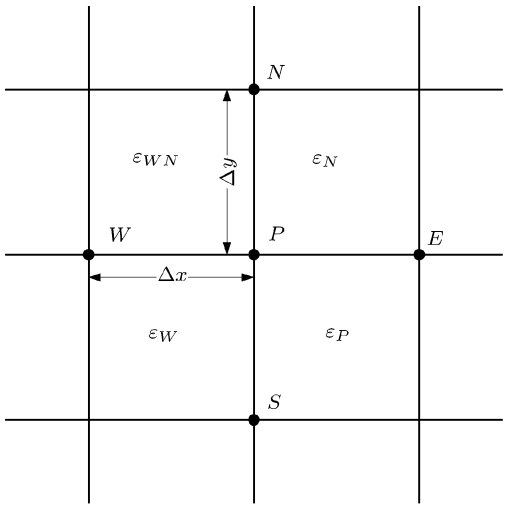


Fig.2. Point P and its neighbouring points in a Cartesian mesh.

To derive the difference equations based on Eqs.(6) and (7), we substitute the second derivatives $\partial^2 H^P_{x,y}/\partial y^2$ and $\partial^2 H^P_{x,y}/\partial y^2$ by a second-order Taylor series expansion at point P. Three sets of two $H_x - H_y$ coupled equations can be obtained, which are about points E, S, P, points W, S, P and points E, N, P. The six equations are expressed as follows:

$$\frac{2}{h_x^2}\left(H_E^x - H_P^x - h_x \left.\frac{\partial H_P^x}{\partial x}\right|_E\right) + \frac{2}{h_y^2}\left(H_S^x - H_P^x - h_y \left.\frac{\partial H_P^x}{\partial y}\right|_S\right) + \frac{1}{\varepsilon_P}\frac{\partial \varepsilon_P}{\partial y}\left(\left.\frac{\partial H_P^y}{\partial x}\right|_E - \left.\frac{\partial H_P^x}{\partial y}\right|_S\right) + k_0^2 \varepsilon_P H_P^x = \beta^2 H_P^x, \tag{8}$$

$$\frac{2}{h_x^2}\left(H_E^y - H_P^y - h_x \left.\frac{\partial H_P^y}{\partial x}\right|_E\right) + \frac{2}{h_y^2}\left(H_S^y - H_P^y - h_y \left.\frac{\partial H_P^y}{\partial y}\right|_S\right) - \frac{1}{\varepsilon_P}\frac{\partial \varepsilon_P}{\partial y}\left(\left.\frac{\partial H_P^y}{\partial x}\right|_E - \left.\frac{\partial H_P^x}{\partial y}\right|_S\right) + k_0^2 \varepsilon_P H_P^y = \beta^2 H_P^y, \tag{9}$$

$$\frac{2}{h_x^2}\left(H_W^x - H_P^x + h_x \left.\frac{\partial H_P^x}{\partial x}\right|_W\right) + \frac{2}{h_y^2}\left(H_S^x - H_P^x - h_y \left.\frac{\partial H_P^x}{\partial y}\right|_S\right) + \frac{1}{\varepsilon_W}\frac{\partial \varepsilon_W}{\partial y}\left(\left.\frac{\partial H_P^y}{\partial x}\right|_W - \left.\frac{\partial H_P^x}{\partial y}\right|_S\right) + k_0^2 \varepsilon_W H_P^x = \beta^2 H_P^x, \tag{10}$$

$$\frac{2}{h_x^2}\left(H_W^y - H_P^y + h_x \left.\frac{\partial H_P^y}{\partial x}\right|_W\right) + \frac{2}{h_y^2}\left(H_S^y - H_P^y - h_y \left.\frac{\partial H_P^y}{\partial y}\right|_S\right) - \frac{1}{\varepsilon_W}\frac{\partial \varepsilon_W}{\partial y}\left(\left.\frac{\partial H_P^y}{\partial x}\right|_W - \left.\frac{\partial H_P^x}{\partial y}\right|_S\right) + k_0^2 \varepsilon_W H_P^y = \beta^2 H_P^y, \tag{11}$$

$$\frac{2}{h_x^2}\left(H_E^x - H_P^x - h_x \left.\frac{\partial H_P^x}{\partial x}\right|_E\right) + \frac{2}{h_y^2}\left(H_N^x - H_P^x + h_y \left.\frac{\partial H_P^x}{\partial y}\right|_N\right) + \frac{1}{\varepsilon_N}\frac{\partial \varepsilon_N}{\partial y}\left(\left.\frac{\partial H_P^y}{\partial x}\right|_E - \left.\frac{\partial H_P^x}{\partial y}\right|_N\right) + k_0^2 \varepsilon_N H_P^x = \beta^2 H_P^x, \tag{12}$$

$$\frac{2}{h_x^2}\left(H_E^y - H_P^y - h_x \left.\frac{\partial H_P^y}{\partial x}\right|_E\right) + \frac{2}{h_y^2}\left(H_N^y - H_P^y + h_y \left.\frac{\partial H_P^y}{\partial y}\right|_N\right) - \frac{1}{\varepsilon_N}\frac{\partial \varepsilon_N}{\partial y}\left(\left.\frac{\partial H_P^y}{\partial x}\right|_E - \left.\frac{\partial H_P^x}{\partial y}\right|_N\right) + k_0^2 \varepsilon_N H_P^y = \beta^2 H_P^y. \tag{13}$$

Then, the properly formulated boundary conditions in x and y direction are derived from Maxwell's equations, which have the following forms:[12]

$$\left.\frac{\partial H_P^x}{\partial x}\right|_W = \left.\frac{\partial H_P^x}{\partial x}\right|_E, \tag{14}$$

$$\frac{1}{\varepsilon_W}\left.\frac{\partial H_P^y}{\partial x}\right|_W - \frac{1}{\varepsilon_P}\left.\frac{\partial H_P^y}{\partial x}\right|_E = \left(\frac{1}{\varepsilon_W} - \frac{1}{\varepsilon_P}\right)\left.\frac{\partial H_P^x}{\partial y}\right|_S, \tag{15}$$

$$\left.\frac{\partial H_P^y}{\partial y}\right|_N = \left.\frac{\partial H_P^y}{\partial y}\right|_S, \tag{16}$$

$$\frac{1}{\varepsilon_N}\left.\frac{\partial H_P^x}{\partial y}\right|_N - \frac{1}{\varepsilon_P}\left.\frac{\partial H_P^x}{\partial y}\right|_S = \left(\frac{1}{\varepsilon_N} - \frac{1}{\varepsilon_P}\right)\left.\frac{\partial H_P^y}{\partial x}\right|_E. \tag{17}$$

With the boundary conditions (14)–(17), Eqs.(8)–(13) are combined and reduced to one set of two coupled equations for H_x and H_y, which can be expressed as eigen-value equation in the form of matrix:

$$\begin{bmatrix} A_{xx} & A_{xy} \\ A_{yx} & A_{yy} \end{bmatrix} \begin{bmatrix} H_x \\ H_y \end{bmatrix} = \beta^2 \begin{bmatrix} H_x \\ H_y \end{bmatrix}, \tag{18}$$

where the differential operators are defined as follows:

$$A_{xx}H_x = \frac{H_W^x + H_E^x}{h_x^2} + \frac{2}{h_y^2}H_S^x - \left[\frac{2}{h_x^2} + \frac{2}{h_y^2} - \frac{k_0^2}{2}(\varepsilon_W + \varepsilon_P)\right]H_P^x + \frac{2(\varepsilon_P + \varepsilon_W) + h_y\frac{\partial \varepsilon_W}{\partial y} - h_x\frac{\partial \varepsilon_W}{\partial x} + h_y\frac{\partial \varepsilon_P}{\partial y} + h_x\frac{\partial \varepsilon_P}{\partial x}}{2(\varepsilon_W + \varepsilon_N) - h_y\frac{\partial \varepsilon_N}{\partial y} - h_x\frac{\partial \varepsilon_W}{\partial x} + h_y\frac{\partial \varepsilon_P}{\partial y} + h_x\frac{\partial \varepsilon_P}{\partial x}}\left[\frac{H_N^x - H_S^x}{h_y^2} + \frac{k_0^2}{2}(\varepsilon_N - \varepsilon_P)H_P^x\right],$$

$$A_{xy}H_y = \frac{\dfrac{2}{h_y}(\varepsilon_P-\varepsilon_N)+\dfrac{\partial\varepsilon_N}{\partial y}+\dfrac{\partial\varepsilon_W}{\partial y}}{2(\varepsilon_W+\varepsilon_N)-h_y\dfrac{\partial\varepsilon_N}{\partial y}-h_x\dfrac{\partial\varepsilon_W}{\partial x}+h_y\dfrac{\partial\varepsilon_P}{\partial y}+h_x\dfrac{\partial\varepsilon_P}{\partial x}}\left[\frac{H_E^y-H_W^y}{h_x}-\frac{h_xk_0^2(\varepsilon_W-\varepsilon_P)}{2}H_P^y\right],$$

$$A_{yx}H_x = \frac{\dfrac{2}{h_x}(\varepsilon_P-\varepsilon_W)+\dfrac{\partial\varepsilon_N}{\partial x}+\dfrac{\partial\varepsilon_W}{\partial x}}{2(\varepsilon_W+\varepsilon_N)-h_y\dfrac{\partial\varepsilon_N}{\partial y}-h_x\dfrac{\partial\varepsilon_W}{\partial x}+h_y\dfrac{\partial\varepsilon_P}{\partial y}+h_x\dfrac{\partial\varepsilon_P}{\partial x}}\left[\frac{H_S^x-H_N^x}{h_y}-\frac{h_yk_0^2(\varepsilon_N-\varepsilon_P)}{2}H_P^x\right],$$

$$\begin{aligned}A_{yy}H_y =& \frac{H_N^y+H_S^y}{h_y^2}+\frac{2}{h_x^2}H_E^x-\left[\frac{2}{h_x^2}+\frac{2}{h_y^2}-\frac{k_0^2}{2}(\varepsilon_N+\varepsilon_P)\right]H_P^y\\ &+\frac{2(\varepsilon_P+\varepsilon_N)-h_y\dfrac{\partial\varepsilon_N}{\partial y}+h_x\dfrac{\partial\varepsilon_N}{\partial x}+h_y\dfrac{\partial\varepsilon_P}{\partial y}+h_x\dfrac{\partial\varepsilon_P}{\partial x}}{2(\varepsilon_W+\varepsilon_N)-h_y\dfrac{\partial\varepsilon_N}{\partial y}-h_x\dfrac{\partial\varepsilon_W}{\partial x}+h_y\dfrac{\partial\varepsilon_P}{\partial y}+h_x\dfrac{\partial\varepsilon_P}{\partial x}}\\ &\times\left[\frac{H_W^y-H_E^y}{h_x^2}+\frac{k_0^2}{2}(\varepsilon_W-\varepsilon_P)H_P^y\right].\end{aligned} \tag{19}$$

Equations (18) and (19) can be numerically solved by LAPACK subroutines.[13] The Dirichlet condition is introduced to approximate the points on the edge of calculation region, which can avoid the nonphysical reflection.[8,14]

The corresponding electric fields of eigen-modes in channel waveguide then can be obtained by substituting the simulated magnetic fields into following equations derived from Maxwell's equations:

$$\begin{aligned}E_x &= \frac{1}{ck_0\varepsilon_0\varepsilon}\left[\beta H_y-\frac{1}{\beta}\left(\frac{\partial^2H_x}{\partial x\partial y}+\frac{\partial^2H_y}{\partial y^2}\right)\right],\\ E_y &= \frac{1}{ck_0\varepsilon_0\varepsilon}\left[-\beta H_x+\frac{1}{\beta}\left(\frac{\partial^2H_y}{\partial x\partial y}+\frac{\partial^2H_x}{\partial x^2}\right)\right],\end{aligned} \tag{20}$$

where c and ε_0 are the velocity of light and electric permittivity in vacuum, respectively.

3. Results and discussions

In the simulations, the calculation region is the combination of air cladding and glass substrate layers, which are composed of rectangular meshes in the domain of [–20 μm, 20 μm] × [–5 μm, 0] and [–20 μm, 20 μm] × [0, 30 μm], respectively; Δx and Δy both equal 0.1 μm. For the parameters used in simulations, n_s=1.530, n_{Ag}=0.025, D_{Ag}=6×10^{-16} m^2/s and α = 0.1, we relied on values reported in the Refs.[4, 15, 16]. These chosen parameters do not correspond to any particular glass substrate, but are typical for buried channel waveguides of graded index profile fabricated by Ag^+–Na^+ ion exchange on EDG.

In EDWA, guided lightwaves of 980 and 1550-nm wavelengths are the typical pump and signal light, respectively. Figure 3 shows the simulated magnetic fields of signal light. The COW is 8 μm, and represented by the line w_1w_2 in Fig.3. T_1 and T_2/T_1 (T_2 is the time-length of second step ion exchange) are 3 hours and 0.5, respectively. The dashed lines in the figures are contours of index profiles of channel waveguide. There are only fundamental modes (Figs.3(a)–3(d)) for signal light in the channel waveguide. The fundamental modes contain two hybrid modes with different polarizations, which are HE (Figs.3(a) and 3(b)) and EH (Figs.3(c) and 3(d)) polarization modes, respectively. The major components of the two polarization modes (H_y for the HE polarization and H_x for the EH polarization) are similar in the distribution profile. This suggests that the polarization dependent loss of waveguide will be low. Except major components, the minor components (H_x for the HE polarization and H_y for the EH polarization) are also observed. The amplitudes of minor components are about 2 to 3 orders weaker than those of major components. The evident hybrid nature of eigen-modes is caused by the intercoupling between H_x and H_y in graded index channel waveguide, and varied with the wavelength of guided wave. It can only be revealed by full-vectorial method. From Fig.3, we find that the minor components behave differently for HE and EH polarization modes. This can be explained by the fact that the index profile of channel waveguide is quasi-ellipse as shown by the dashed lines in Fig.3.

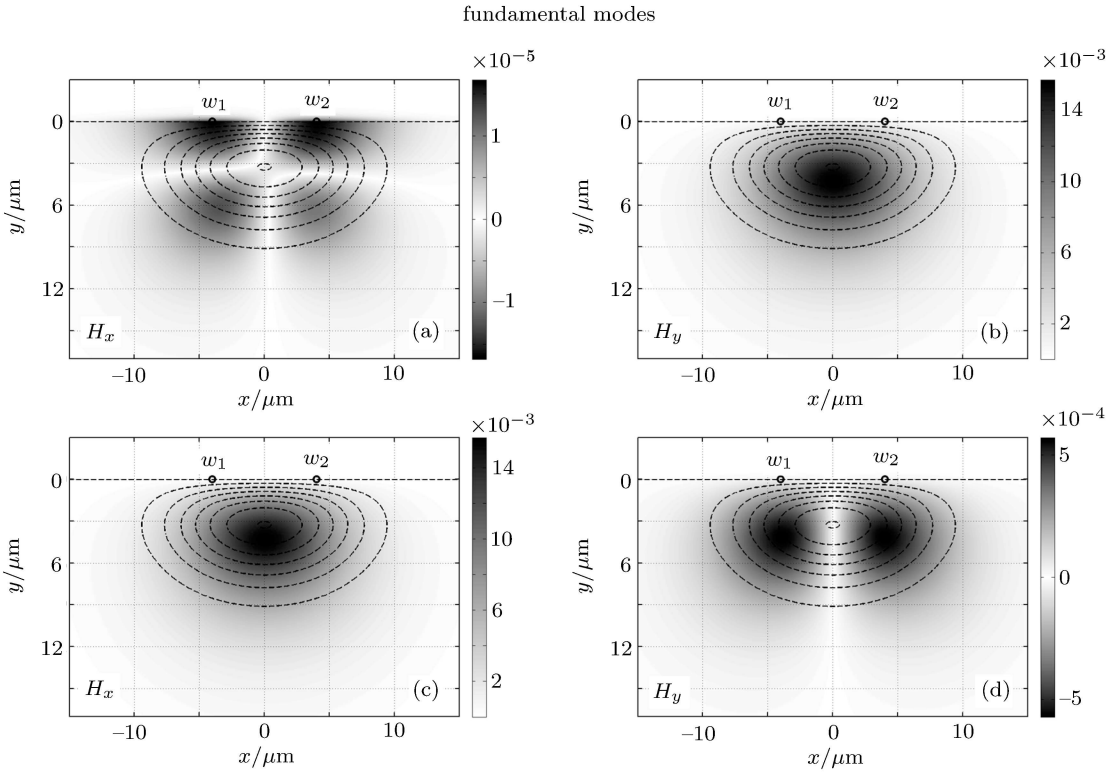
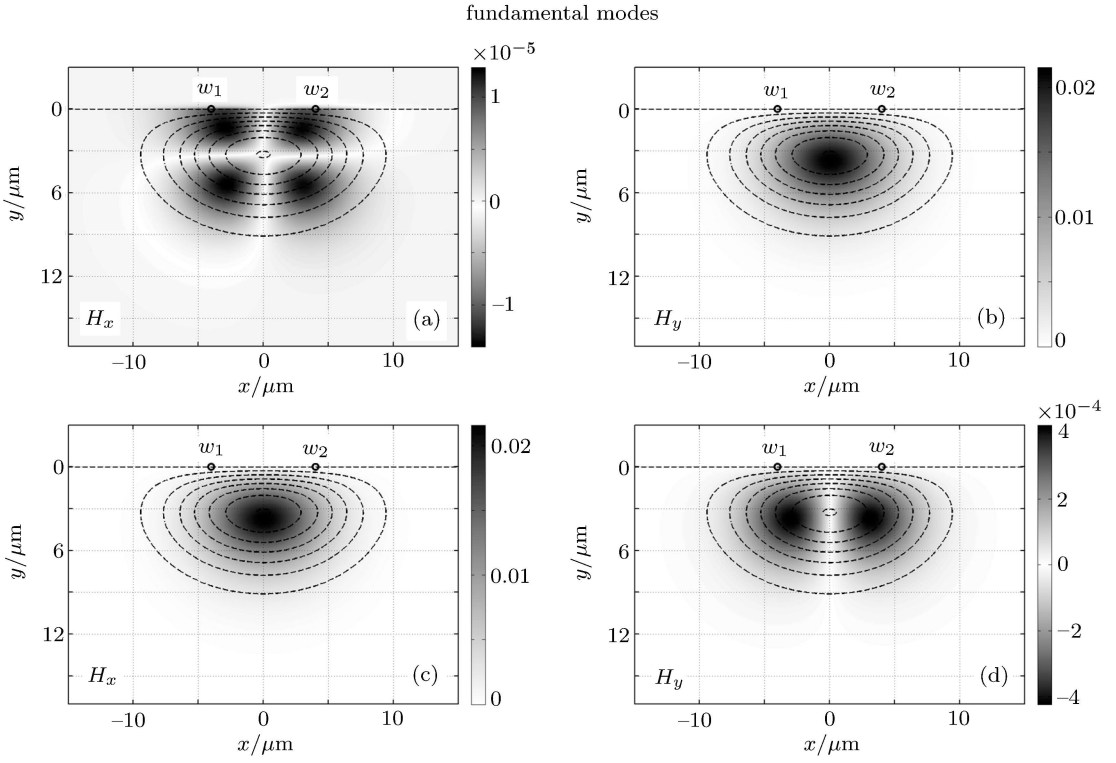


Fig.3. Normalized magnetic field patterns of signal light (1550 nm) with COW=8 μm (distance between w_1 and w_2). Dashed lines are the contours of index profile of waveguide.

Figure 4 shows the numerical magnetic fields of pump light. The simulation parameters are the same as those used for signal light. According to the profile of major component, the eigen-modes of pump light in Fig.4 can be divided into three groups, which are fundamental modes (Figs.4(a)–4(d)), first order modes (Figs.4(e)–4(h)) and second order modes (Figs.4(i)–4(l)). Each group of modes contains HE (upper row in the group) and EH (lower row in group) polarization modes. Comparing the results in Fig.4 with those



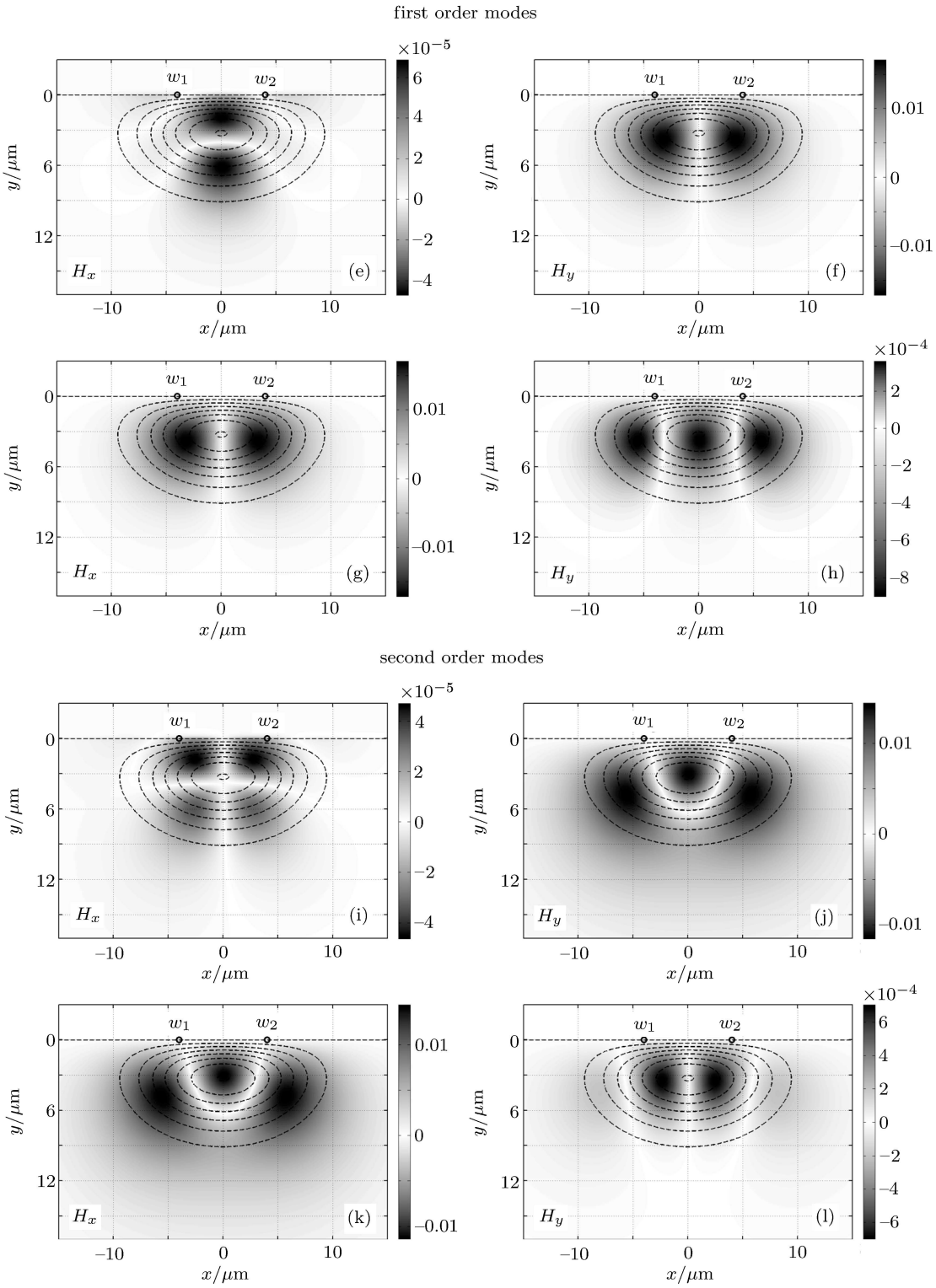


Fig.4. Normalized magnetic field patterns of pump light (980 nm) with COW=8 μm (distance between w_1 and w_2). Dashed lines are the contours of index profiles of waveguide.

in Fig.3, we find that the pump light becomes multimode while the signal light maintains monomode for the same waveguide. The suppression of higher order mode in Fig.3 contributes to the longer wavelength of signal light. In EDWA, it is inevitable for pump light to operate at multimode status when we make sure it is monomode signal light at *C*-band. The requirement of monomode signal light should be met in the design and fabrication of EDW in order to make EDWA adapted to the optical fibre communication

system.

Figure 5 shows the maximal index of waveguide layer ($n_{\max}$), effective index of eigen-modes (N_i) and section area of fundamental mode (S_0) versus COW. T_1 and T_2/T_1 are fixed to 3 hours and 0.7, respectively. S_0 is defined as the area where the magnetic field is larger than $1/e$ of its peak value for the major component of fundamental mode. Figures 5(a) and 5(b) show the simulated results of pump light and signal light, respectively. It is obvious that N_i of HE and EH polarization modes with the same order are almost the same for various COW. This means that low polarization dependent loss for both signal and pump light can be achieved in channel waveguides fabricated by ion exchange technique. Results also show that $n_{\max}$ and the eigen-mode number of pump light increase with the increase of COW. And the signal light can maintain monomode for channel waveguide fabricated using these parameters. The grey curves in Fig.5 show

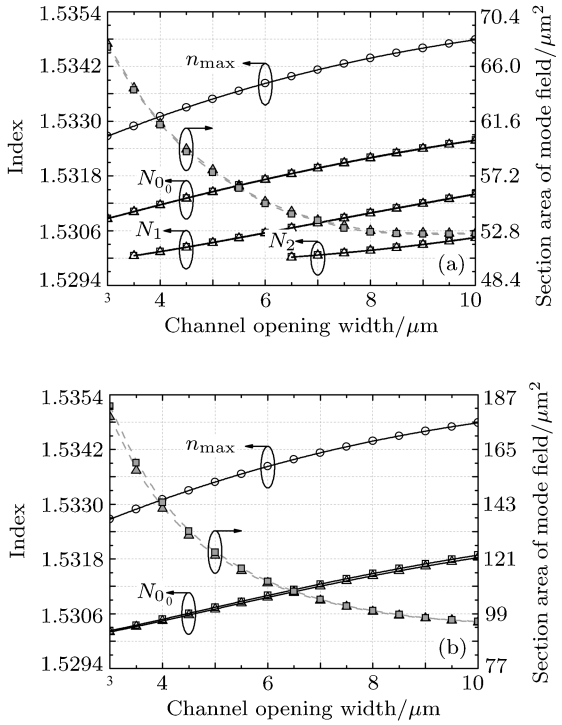


Fig.5. Effective index of eigen-modes in waveguide and section area of fundamental mode versus COW. (a) pump light (980 nm), (b) signal light (1550 nm). Solid line with open circle denotes the maximal index of waveguide layer. Square symbols represent HE polarization modes and triangle symbols the EH polarization modes. Dashed lines with grey solid symbols □ or △ denote section area of fundamental mode. Solid lines with □ or △ are effective index of eigen-modes in waveguide, and N_i is the order of eigen-modes.

that S_0 of both pump and signal light decrease with the increase of COW. This can be explained by the fact that guided wave will be focused when $n_{\max}$ becomes higher.

Figure 6 presents $n_{\max}$, N_i and S_0 versus T_2/T_1. T_1 and COW are fixed to 3 hours and 7 μm, respectively. Figures 6(a) and 6(b) show the simulated results of pump light and signal light, respectively. The parameter T_2/T_1 is mainly used to control the buried depth of channel waveguide and the symmetry of index profile in two-step ion exchange process. We find that $n_{\max}$ decreases when T_2/T_1 increases. This causes the reduction of eigen-mode number and the increase of S_0 for both pump and signal light.

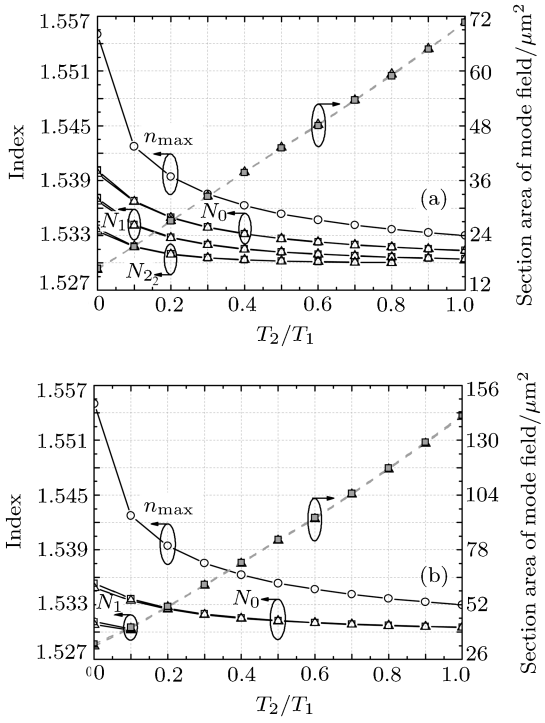


Fig.6. Effective index of eigen-modes in waveguide and section area of fundamental mode versus time ratio of the second step to first step in ion exchange: (a) pump light (980 nm), (b) signal light (1550 nm). Solid lines with open circles denote maximal index of waveguide layer, square symbols the HE polarization modes and triangle symbols the EH polarization modes. Dashed lines with grey solid symbols □ or △ denote section area of fundamental mode. Solid lines with □ or △ denote effective index of eigen-modes in waveguide, and N_i the order of eigen-modes.

From the results in Figs.5 and 6, we can find that the fabrication parameters of COW and T_2/T_1 both have large influence on the properties of channel waveguide, such as the number of eigen-modes and section area of fundamental mode. In EDWA, the net gain will be enhanced with the increase of $\Gamma_{\mathrm{p,s}}$, which can be achieved by raising the mode confinement in active region.[2] As the Er^{3+} ions are doped uniformly all over the substrate glass, COW and T_2/T_1 should

be well chosen to confine the section area of fundamental mode in channel waveguide, which can improve the gain dynamics of EDWA. In addition, the coupling loss between monomode fibre and channel waveguide, which is caused by the mode mismatch, is usually taken into account. Thus, COW and T_2/T_1 should also be limited to maintain the monomode for channel waveguide when signal light is propagating. In this way, the optimization of parameters such as COW and T_2/T_1 is significant in the design and fabrication of EDWA with ion exchange technique.

Further simulations show that it is possible for the waveguide to propagate monomode signal light of only HE polarization, which does not contain EH polarization. From the above numerical results we can conclude that number of eigen-modes decreases with the increase of light wavelength. When using the parameters such as T_1=3 hours, T_2/T_1=1 and COW=3 μm, we find that the cutoff wavelengths for EH and HE polarized fundamental modes are 1528 nm and 1541 nm, respectively. Thus, there exists about 13-nm bandwidth from 1528 to 1541 nm at C-band for the waveguide to propagate only HE polarization fundamental mode. The working bandwidth of single polarization EDWA will become about 14 nm from 1571 to 1585 nm at L-band when COW is expanded to 3.2 μm. The simulated results suggest that both single polarization EDWA and polarization independent EDWA can be achieved by ion exchange technique.

4. Conclusions

A general numerical tool, based on thermal diffusion equation and full-vectorial eigen-mode equation, has been presented for the systematic analysis of graded index channel waveguide fabricated by ion exchange on EDG. FV-FDM is applied to solving the full-vectorial modes of graded index channel waveguide. The coupled difference equations based on magnetic fields in FV-FDM are derived from the Taylor series expansion and accurate formulation of boundary conditions. FV-FDM provides an accurate electromagnetic analysis on the mode distribution in graded index channel waveguide. The hybrid nature of vectorial guided modes for both pump and signal light is demonstrated by the simulation. The effective index and distribution of eigen-modes for the channel waveguides fabricated with different parameters, such as COW and T_2/T_1, are numerically analysed. Results also show that these parameters have large influence on the properties of waveguide. By optimizing the fabrication parameters, maintenance of monomode for signal light and improvement of the gain dynamics can be achieved in EDWA fabricated by ion exchange technique. This theoretical model is significant for the design and fabrication of EDWA with ion exchange technique. Furthermore, we numerically design a single polarization EDWA, which operates at the wavelength from 1528 to 1541 nm for HE polarization. And the working wavelength can be changed with the fabrication parameters.

References

[1] Tan N and Zhang Q Y 2006 *Chin. Phys.* **15** 2165

[2] Ke L and Edwin Y B Pun 2007 *Opt. Commun.* **273** 413

[3] Jose G, Sorbello G, Taccheo S, Cianci E, Foglietti V and Laporta P 2003 *J. Non-Cryst. Solids* **332** 256

[4] West B R, Madasamy P, Peyghambarian N and Honkanen S 2004 *J. Non-Cryst. Solids* **347** 18

[5] Miliou A, Zhenguang H, Cheng H C, Srivastava R and Ramaswamy R V 1989 *IEEE J. Quantum Electron.* **25** 1889

[6] Lou N, Jin G L, Gu H R and Li Q 2007 *Opt. Eng.* **46** 044601

[7] Scarmozzino R, Gopinath A, Pregla R and Helfert S 2000 *IEEE J. Sel. Topics Quantum Electron.* **6** 150

[8] Xiao J B, Zhang M D and Sun X H 2006 *Chin. Phys.* **15** 143

[9] Chiang Y C, Chiou Y P and Chang H C 2002 *J. Lightw. Technol.* **20** 1609

[10] Magnus Wik, Derek Dumas and David Yevick 2005 *J. Opt. Soc. Am.* A **22** 1341

[11] Wiliam J Layton and Patrick J Rabier 2005 *Numerical Linear Algebra with Applications* **2** 363

[12] Lüsse P, Stuwe P, Schüle J and Unger H G 1994 *J. Lightw. Technol.* **12** 487

[13] Aderson E, Bai Z, Bischof E, Blackford L S, Demmel J, Dongarra J J, Croz J D, Hammarling S, Greenbaum A, Mckenney A and Sorensen A 1999 *LAPACK Users Guide* 3rd edn (Philadelphia: SIAM)

[14] Kenji Kawano and Tsutonu Kitoh 2001 *Introduction to Optical Waveguide Analysis* (New York: Wiley)

[15] Jerome Hazart and V Minier 2001 *IEEE J. Quantum Electron.* **37** 606

[16] Jin G L, Shao G W, Mu H, Hu L L and Li Q 2005 *Chin. Phys. Lett.* **22** 2862